

$\beta$ -delayed three-proton decay of  $^{31}\text{Ar}$ 

A.A. Lis,<sup>1</sup> C. Mazzocchi,<sup>1,\*</sup> W. Dominik,<sup>1</sup> Z. Janas,<sup>1</sup> M. Pfützner,<sup>1,2</sup> M. Pomorski,<sup>1</sup> L. Acosta,<sup>3,4</sup> S. Baraeva,<sup>5</sup> E. Casarejos,<sup>6</sup> J. Duénas-Díaz,<sup>7</sup> V. Dunin,<sup>5</sup> J. M. Espino,<sup>8</sup> A. Estrade,<sup>9</sup> F. Farinon,<sup>2</sup> A. Fomichev,<sup>5</sup> H. Geissel,<sup>2</sup> A. Gorshkov,<sup>5</sup> G. Kamiński,<sup>10,11</sup> O. Kiselev,<sup>2</sup> R. Knöbel,<sup>2</sup> S. Krupko,<sup>5</sup> M. Kuich,<sup>1,12</sup> Yu. A. Litvinov,<sup>2</sup> G. Marquinez-Durán,<sup>7</sup> I. Martel,<sup>7</sup> I. Mukha,<sup>2</sup> C. Nociforo,<sup>2</sup> A.K. Ordúz,<sup>7</sup> S. Pietri,<sup>2</sup> A. Prochazka,<sup>2</sup> A.M. Sánchez-Benítez,<sup>7,13</sup> H. Simon,<sup>2</sup> B. Sitar,<sup>14</sup> R. Slepnev,<sup>5</sup> M. Stanoiu,<sup>15</sup> P. Strmen,<sup>14</sup> I. Szarka,<sup>14</sup> M. Takechi,<sup>2</sup> Y. Tanaka,<sup>2,16</sup> H. Weick,<sup>2</sup> and J.S. Winfield<sup>2</sup>

<sup>1</sup>*Faculty of Physics, University of Warsaw, 02-093 Warszawa, Poland*

<sup>2</sup>*GSI Helmholtzzentrum für Schwerionenforschung, 64291 Darmstadt, Germany*

<sup>3</sup>*INFN, Laboratori Nazionali del Sud, Via S. Sofia, Catania, Italy*

<sup>4</sup>*Instituto de Física, Universidad Nacional Autónoma de México, México D. F. 01000, Mexico.*

<sup>5</sup>*Joint Institute for Nuclear Research, 141980 Dubna, Russia*

<sup>6</sup>*University of Vigo, 36310, Vigo, Spain*

<sup>7</sup>*Department of Applied Physics, University of Huelva, 21071 Huelva, Spain*

<sup>8</sup>*University of Seville, 41012 Seville, Spain*

<sup>9</sup>*University of Edinburgh, EH1 1HT Edinburgh, United Kingdom*

<sup>10</sup>*Institute of Nuclear Physics PAN, 31-342 Kraków, Poland*

<sup>11</sup>*Joint Institute for Nuclear Research, 141980 Dubna, Moscow Region, Russia*

<sup>12</sup>*Faculty of Physics, Warsaw University of Technology, 00-662 Warszawa, Poland*

<sup>13</sup>*Centro de Física Nuclear da Universidade de Lisboa, 1649-003 Lisboa, Portugal*

<sup>14</sup>*Faculty of Mathematics and Physics, Comenius University, 84248 Bratislava, Slovakia*

<sup>15</sup>*IFIN-HH, Post Office Box MG-6, Bucharest, Romania*

<sup>16</sup>*University of Tokyo, Japan*

(Dated: April 23, 2022)

The  $\beta$  decay of  $^{31}\text{Ar}$ , produced by fragmentation of a  $^{36}\text{Ar}$  beam at 880 MeV/nucleon, was investigated. Identified ions of  $^{31}\text{Ar}$  were stopped in a gaseous time projection chamber with optical readout allowing to record decay events with emission of protons. In addition to  $\beta$ -delayed emission of one and two protons we have clearly observed the  $\beta$ -delayed three-proton branch. The branching ratio for this channel in  $^{31}\text{Ar}$  is found to be  $0.07 \pm 0.02\%$ .

PACS numbers: 23.40.-s, 23.50.+Z, 27.30.+t

## I. INTRODUCTION

Nuclides at the proton drip-line are characterised by large  $\beta^+$ -decay  $Q$  values which allow population of particle-unbound states in the daughter nuclei. This makes the process of  $\beta$ -delayed (multi) particle emission possible [1, 2]. The probability of this phenomenon becomes particularly sizeable when the isobaric analogue state (IAS) is located above the respective threshold. The  $\beta$ -delayed single proton emission ( $\beta p$ ), studied intensively over the last 50 years, has provided a wealth of information on the structure of neutron-deficient nuclei [1]. The delayed emission of two protons ( $\beta 2p$ ), discovered in 1983 [3], now is known to occur in 11 cases [1, 4]. The interesting additional aspect of this decay mode is the mechanism of two-proton emission which could proceed either sequentially or simultaneously. Much less is known on delayed emission of more than two particles. Prior to the study reported in this paper only two cases of  $\beta$ -delayed three-proton emission ( $\beta 3p$ ) were known:  $^{45}\text{Fe}$  [5] and  $^{43}\text{Cr}$  [6]. Both of them were observed with help of a very sensitive gaseous detector — the Optical Time

Projection Chamber (OTPC) — which records tracks of charged particles in space. With this approach a single good event is sufficient to establish a new decay channel. In this paper we report the observation of the third case of  $\beta 3p$  decay,  $^{31}\text{Ar}$ , accomplished with this technique.

The most neutron-deficient argon isotope known to date,  $^{31}\text{Ar}$ , was observed for the first time almost 30 years ago [7]. It decays with the half-life of  $T_{1/2} = 15.1(3)$  ms [8] and the energy  $Q_{EC} = 18.3(2)$  MeV [9]. In such a large decay-energy window many channels for delayed emission of protons are open. In fact,  $^{31}\text{Ar}$  is the most extensively studied case of  $\beta 2p$  decay [10–14]. In addition, it was considered as a primary candidate for the  $\beta 3p$  decay and the search for this decay mode has an interesting history. Already in 1992 Bazin et al. claimed the first observation of this channel in  $^{31}\text{Ar}$  [15]. In an experiment performed at GANIL Caen with  $^{31}\text{Ar}$  ions implanted into a segmented silicon detector, the branching ratio for  $\beta 3p$  channel was claimed to be  $\beta 3p = 2.1(10)\%$  [15]. However, a measurement made later at CERN-ISOLDE, employing a silicon detector array of larger granularity and efficiency, failed to observe this decay mode. Only an upper limit for the  $\beta 3p$  decay branch from the IAS state in  $^{31}\text{Cl}$  to the ground state of  $^{28}\text{Si}$  was deduced to be 0.11% [16].

\* chiara.mazzocchi@fuw.edu.pl

Motivated by the success of applying the OTPC detector to studies of  $\beta$ -delayed multiparticle emission [5, 6], we have used it to investigate the delayed particles emitted in the decay of  $^{31}\text{Ar}$ . The preliminary results, demonstrating clear and unambiguous evidence for the  $\beta 3p$  events, were presented in Ref. [17]. Soon afterwards, the reanalysis of data collected previously at CERN-ISOLDE fully supported this observation [8, 18]. Here we present results of the complete analysis of our experiment.

## II. EXPERIMENTAL TECHNIQUE

The experiment was performed at the GSI Helmholtzzentrum für Schwerionenforschung, Darmstadt, Germany. The  $^{31}\text{Ar}$  ions were produced in the fragmentation reaction of a  $^{36}\text{Ar}$  primary beam at 880 MeV/nucleon impinging on a 8 g/cm<sup>2</sup> beryllium target. The  $^{31}\text{Ar}$  fragments were separated by the Fragment Separator (FRS) [19]. The setting of the FRS was not the standard one. Instead, the first half of the separator was used to select and form the secondary beam of  $^{31}\text{Ar}$  using a 5 g/cm<sup>2</sup> thick aluminum degrader located at the S1 focal plane which was shaped for achromatic focusing to the intermediate focal plane (S2). There this beam was impinging on a secondary target for a purpose of a different experiment which will be reported elsewhere. The unreacted ions of  $^{31}\text{Ar}$  were transported through the second half of the FRS to the final focal plane (S4). There, after passing through the standard FRS detectors, the ions were slowed down by a variable aluminum degrader, and entered our detection system based of the gaseous Optical Time Projection Chamber (OTPC). In front of the OTPC entrance window a  $30 \times 30$  mm<sup>2</sup>, 300  $\mu\text{m}$  thick silicon detector was mounted and an additional variable aluminum degrader to optimize the implantation of selected ions was installed.

The OTPC was developed at the University of Warsaw, primarily to study rare decay processes with emission of charged particles, like 2p radioactivity [20, 21]. The unit used in the present study was described in some details in Ref. [4]. Here we give only the main features and those details which are specific to the reported experiment. The active volume of the chamber was filled with a gas mixture of 98 % Ar and 2 % N<sub>2</sub> at atmospheric pressure. The fiducial length of the detector was 31 cm. A uniform, vertical electric drift field of 300 V/cm was maintained inside the chamber. Primary ionization electrons, generated by incoming ions and their charged decay products, were drifting towards the charge amplification stage made by a stack of four GEM foils [22] and a wire mesh anode. Before reaching the anode, the electrons stimulate the gas atoms to emit light. This light was detected by a CCD camera and a photomultiplier tube (PMT). The CCD image provided a projection of the particles tracks on the horizontal plane integrated over the exposure time. The PMT signal, sampled by a digital oscilloscope, gives the total intensity of light

as a function of time. This provides information on the time sequence of recorded events. In addition, when the drift velocity of electrons in the given field and gas mixture is known, the vertical coordinate can be determined. Then, by combining data from the CCD and the PMT, the track of a particle can be reconstructed in three dimensions [4, 20].

The detector could operate in a low- or a high-sensitivity mode depending on the potential applied to a special gating electrode mounted between the active volume and the amplification stage. In the low-sensitivity mode the detector is protected against large charges generated by heavy ions. Within 100  $\mu\text{s}$  from the triggering signal, the mode was switched to high sensitivity, optimal for less ionising particles like protons [4]. After the exposure the detector was returned to the low-sensitivity mode.

Ions arriving to the OTPC were identified in-flight using the time-of-flight (TOF) and the energy-loss ( $\Delta E$ ) information. The TOF was measured by means of plastic scintillators mounted at the S2 and the S4 focal planes of the FRS. Each scintillator was read from the left (L) and the right (R) side with respect to the beam axis. Two signals were formed by means of time-to-amplitude (TAC) converters, corresponding to the time between left (LL) and right (RR) readouts. The energy loss ( $\Delta E$ ) was measured by the silicon detector in front of the OTPC. These three identification signals were sampled by a digital oscilloscope and their waveforms were stored. Later, in the off-line analysis the amplitudes of these signals were determined and the average of both TOF values was taken as the final time-of-flight value for the ion.

In order to reduce the amount of data collected, a selective trigger based on the identification information was applied. The trigger signal was generated only by those ions for which the  $\Delta E$  and one of the TAC signals exceeded certain preset amplitudes. The identification plot for ions which triggered the OTPC acquisition system is shown in Fig. 1a. In all previous experiments with the OTPC system, the beam was turned off upon receiving the triggering signal to protect the detector from other ions entering the active volume in the high sensitivity mode. In this experiment such a protection was not possible due to the acceleration scheme of the SIS synchrotron. The primary beam was impinging on the target in 1 s long spills slowly extracted from the SIS. Thus, the reaction products passing through the FRS were coming in bunches correlated with these spills. When the triggering ion arrived, all following ions from the same bunch could enter the OTPC in the high sensitivity mode within the exposure time. The identification signals for all such ions, in addition to the triggering ion, were recorded. Fig. 1b shows the identification plot for all ions which entered the OTPC during the total exposure time, including the triggering ions.

Tracks of the ions which entered the OTPC after the trigger were "contaminating" the CCD image and could obscure the decay events of the stopped  $^{31}\text{Ar}$  ions. In or-

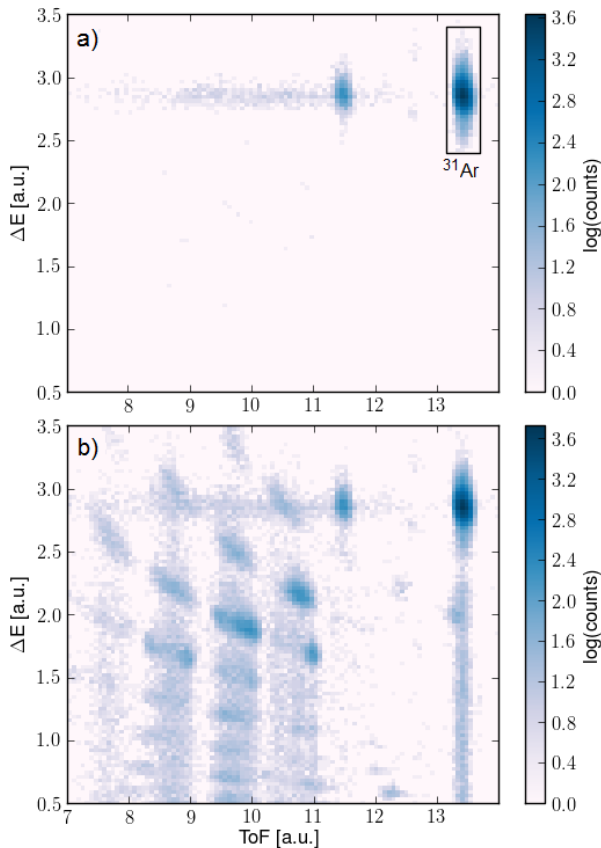


FIG. 1. The  $\Delta E$ -ToF identification plots for ions arriving to the OTPC detector. a) Only the ions which triggered the data acquisition system. The rectangular box shows the gate used to select the  $^{31}\text{Ar}$  events for further analysis. b) All ions recorded by the OTPC during the experiment.

der to remedy this problem and to reduce the number of particle tracks on CCD images, we have applied a special acquisition mode by dividing the full CCD exposure into five shorter frames. The CCD camera was working in the "movie"-like mode, taking continuously subsequent images with a constant exposure time of 16 ms. The dead-time between two consecutive frames due to read-out was 0.79 ms. When the trigger signal arrived, five consecutive frames, starting with the one in which the triggering ion was present, were validated and stored. After the entire exposure lasting 80 ms all the collected data were written to a PC hard disk. The data for each event consisted of five CCD images, the PMT waveform, the three waveforms of the identification signals and the camera readout signal marking the starting time of each CCD frame. An example set of five CCD images collected for one event, picturing the  $\beta 3p$  decay of  $^{31}\text{Ar}$ , is presented in Fig. 2.

### III. ANALYSIS AND RESULTS

Events corresponding to the ions of  $^{31}\text{Ar}$  which triggered the OTPC acquisition were selected by the software gate indicated by a rectangle in Fig. 1a. The total number of such triggers during the data-taking time of five days was about 53000. However, as a result of the high-energy fragmentation reaction and the large thickness of all materials in the beam (target, degraders) the range straggling of the reaction products was much larger than the effective thickness of the OTPC detector. For the further analysis we have selected only those events in which the triggering  $^{31}\text{Ar}$  ion was stopped inside the detector, between 10% and 90% of its length. The latter limits were applied to make sure that all decays with emission of protons will be clearly visible on the CCD image. In addition, only those events were taken into account where on the first CCD frame no other ions than  $^{31}\text{Ar}$  were present. This measure was taken to avoid any ambiguity in the assignment of the decay event to the implanted ion. Finally, this procedure yielded about 21000 events representing the proper implantation of a  $^{31}\text{Ar}$  ion.

Each event was inspected individually. The decay events picturing the emission of a proton or a simultaneous emission of two and three protons were clearly observed. Example events of these three categories are shown in Fig. 3. If the decay was captured on a different CCD frame than the implantation, it was accepted only when the coordinates of the decay vertex on the CCD image coincided with those of the point of implantation. In addition, in case of emission of two and three protons it was verified that the corresponding PMT waveform was consistent with the scenario that all protons were emitted simultaneously, representing a single decay event. The analysis yielded 13157 events of  $\beta p$ , 1729 events of  $\beta 2p$ , and 13 events of  $\beta 3p$ . In the remaining events no decay signals were observed. In these cases either the decay occurred without emission of a proton, or the delayed proton(s) were emitted during the dead-time of the system or after the full exposure time. Due to the finite measuring time and the dead-time between frames, the average probability to observe a decay in the five-frame time-window was 92.3%. This value together with the number of decays allowed to determine the total branching ratios for all the decay channels observed. The results are collected in Table I.

The determined branching ratios for the  $\beta 1p$  and  $\beta 2p$  decays are in agreement with the literature values of 62(2)% and 8.5(4)% [23]. The uncertainties of our values are smaller which illustrates the advantage of the OTPC detector for this kind of studies. Our results are obtained by a simple counting of individual events which are unambiguously identified. No normalisations are involved.

The classification of 13 events as  $\beta 3p$  decays was established with high confidence. It might have happened, however, that some additional events of this type were misclassified as  $\beta 2p$  decays. This could happen if the topology of the decay was particularly unfortunate, for

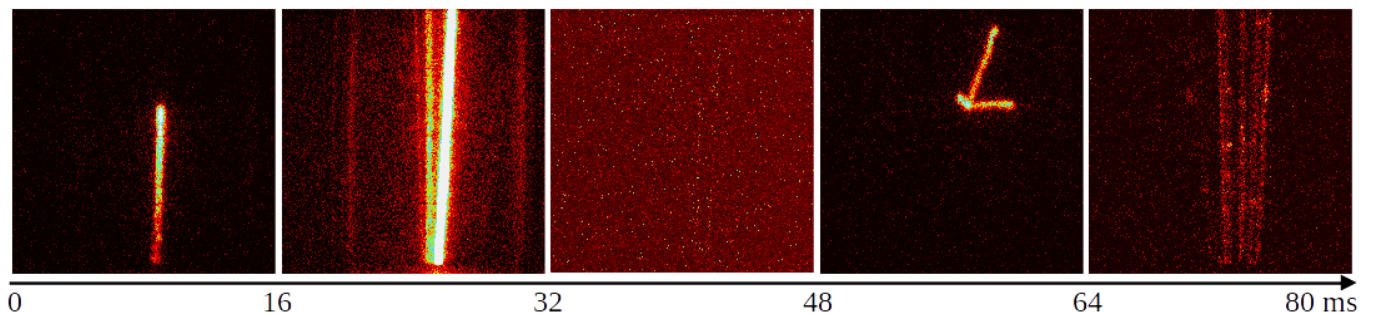


FIG. 2. (Color online) Example set of five consecutive CCD frames collected for one event. Each frame was exposed for 16 ms. In the first frame the track of an implanted  $^{31}\text{Ar}$  ion is visible. In the second and in the fifth frames tracks of contaminant ions passing through the chamber are seen, while on the third frame nothing of interest happened. In the fourth frame the decay of the implanted ion by emission of three  $\beta$ -delayed protons is captured.

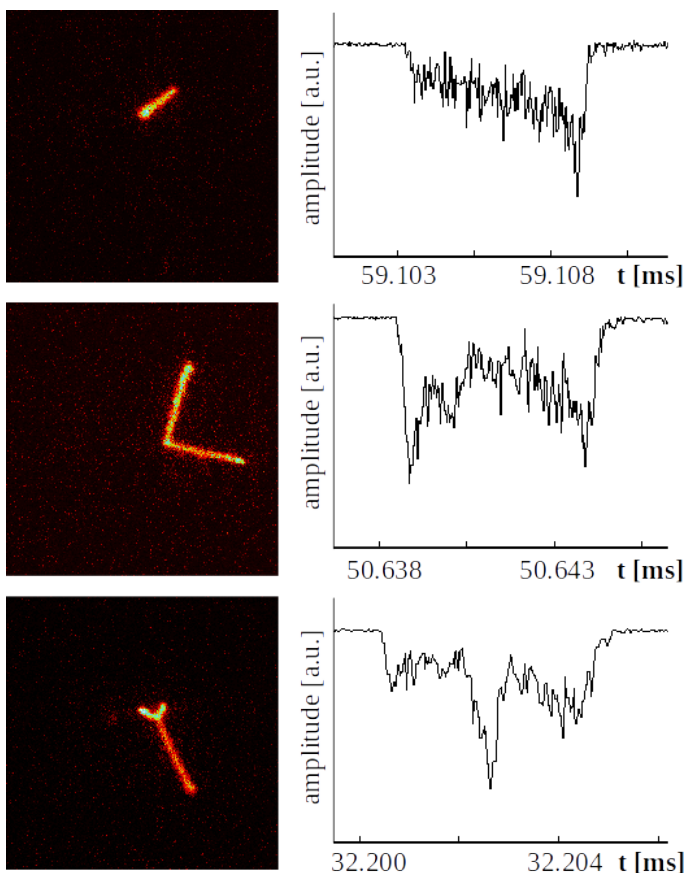


FIG. 3. (Color online) Example events of  $\beta$ -delayed proton emission from  $^{31}\text{Ar}$ . In the left column the CCD images of emitted particles are shown, while the corresponding PMT waveforms are presented in the right column. Examples of  $\beta p$ ,  $\beta 2p$ , and  $\beta 3p$  decays are shown in the top, the middle, and the bottom row, respectively.

example, if one of the protons was emitted along the direction of the electric field and its trace on the PMT waveform was obscured by signals from remaining protons. Since it is difficult to estimate the probability of such scenario, we give only the statistical uncertainty

TABLE I. The total branching ratios for the observed decays of  $^{31}\text{Ar}$ . The given uncertainties are statistical.

Channel	Events	Branching [%]
$\beta 0p$	5984	22.6(3) <sup>a</sup>
$\beta 1p$	13157	68.3(3)
$\beta 2p$	1729	9.0(2)
$\beta 3p$	13	0.07(2)

<sup>a</sup> Value obtained by subtracting the sum of the  $\beta 1p$ ,  $\beta 2p$  and  $\beta 3p$  branching ratios from 100%.

to the branching ratio for the  $\beta 3p$  decay. The value of this branching, however, should be considered as a lower limit.

Our value for the  $\beta 3p$  branching is consistent with the upper limit of 0.11% established previously by Fynbo et al. [16]. Recently, Koldste et al. [8] reported the observation of the  $\beta 3p$  channel in  $^{31}\text{Ar}$  in the experiment performed at ISOLDE, where the delayed particles were detected by means of a highly segmented array of DSSSD detectors providing large granularity and efficiency [24]. The branching ratio for the  $\beta 3p$  decay going through the IAS state in  $^{31}\text{Cl}$  to the ground state of  $^{28}\text{Si}$  was determined to be 0.039(19)%. In addition, it was estimated that this number represents roughly half of all  $3p$  emissions, while the rest of them goes through highly-lying states above the IAS. Thus, the total branching observed in Ref. [8] amounts to about 0.08(4)%. Within error bars, this value agrees well with our result.

In principle, from the data measured by the OTPC detector it is possible to reconstruct the energy of an observed particle under condition, however, that the whole track is contained within the fiducial volume [4]. Unfortunately, in the present experiment a large fraction of the delayed protons emitted in the decay of  $^{31}\text{Ar}$  escaped the detector volume. Hence, here we report only on the decay modes and their total branching ratios.

#### IV. SUMMARY

Beta decay of  $^{31}\text{Ar}$  was investigated at the GSI Fragment Separator by means of an optical-readout time-projection chamber. Decay channels with emission of delayed protons were directly and clearly observed. The measured total branching ratios for the  $\beta p$  and  $\beta 2p$  channels were found to be in agreement with the literature data [23]. Thirteen events of the  $\beta 3p$  emission were unambiguously identified, yielding the branching ratio for this decay mode of 0.07(2)%. This result is in good agreement with the value reported recently by Koldste et al. [8].

Although the probability of the  $\beta 3p$  channel is small, it may have a large impact on the  $\beta$  decay strength distribution. This is because the emission of three protons proceeds mainly from highly excited states in the daughter nucleus, including levels above the isobaric analogue state. As estimated in Ref. [18], the  $\beta 3p$  transitions are responsible for about 30% of the total Gamow-Teller strength distribution observed in  $^{31}\text{Ar}$ . For the exhaustive determination of the  $\beta$  decay strength, the complete information on all decay modes, including all channels of delayed particle emission is mandatory.

The experimental technique of recording rare decay events with emission of heavy charged particles by means

of a gaseous OTPC detector, in combination with the in-flight production of very exotic nuclei, proves to be highly efficient and sensitive. Implantation of a single ion, identified in flight, followed by an observation of its decay is in principle sufficient to prove the occurrence of a decay channel. As a consequence the branching ratios are measured with high accuracy. On the other hand, determination of energy in the current version of the OTPC detector is limited and cannot compete with arrays of silicon detectors. Therefore, these two approaches to particle spectroscopy are complementary and both have to be pursued.

#### ACKNOWLEDGEMENTS

The authors would like to thank the GSI staff for the high-quality beam delivered throughout the experiment. This work was partly supported by the Polish National Science Center under contract no. UMO-2011/01/B/ST2/01943. The participants from JINR are grateful for the grant RFBR No. 14-02-00090. A.A. Lis acknowledges support by the Polish Ministry of Science and Higher Education by the grant No. 0079/DIA/2014/43 ("Grant Diamentowy") and M. Pfützner is grateful for a support from the Helmholtz International Center for FAIR (HIC for FAIR).

- 
- [1] B. Blank and M.J.G. Borge, *Progress in Particle and Nuclear Physics* **60**, 403 (2008).
  - [2] M. Pfützner, M. Karny, L.V. Grigorenko, and K. Riisager, *Rev. Mod. Phys.* **84**, 567 (2012).
  - [3] M.D. Cable, et al., *Phys. Rev. Lett.* **50**, 404 (1983).
  - [4] M. Pomorski et al., *Phys. Rev. C* **90**, 014311 (2014).
  - [5] K. Miernik et al., *Phys. Rev. C* **76**, 041304(R) (2007).
  - [6] M. Pomorski et al., *Phys. Rev. C* **83**, 014306(R) (2011).
  - [7] M. Langevin et al., *Nucl. Phys. A* **455**, 149 (1986).
  - [8] G. T. Koldste et al., *Phys. Rev. C* **89**, 064315 (2014).
  - [9] M. Wang et al., *Chin. Phys. C* **36**, 1603 (2012).
  - [10] M.J.G. Borge, et al., *Nucl. Phys. A* **515**, 21 (1990).
  - [11] L. Axelsson, et al., *Nucl. Phys. A* **628**, 345 (1998).
  - [12] L. Axelsson, et al., *Nucl. Phys. A* **634**, 475 (1998).
  - [13] H.O.U. Fynbo et al., *Nucl. Phys. A* **677**, 38 (2000).
  - [14] H.O.U. Fynbo et al., *Nucl. Phys. A* **701**, 394c (2002).
  - [15] D. Bazin et al., *Phys. Rev. C* **45**, 69 (1992).
  - [16] H.O.U. Fynbo et al., *Phys. Rev. C* **59**, 2275 (1999).
  - [17] M. Pfützner et al., GSI-SR2012-PHN-ENNA-EXP-17, GSI Report 2013-1 (2012).
  - [18] G.T. Koldste et al., *Phys. Lett. B* **737**, 383 (2014).
  - [19] H. Geissel et al., *Nucl. Instr. and Methods in Phys. Res. B* **70**, 286 (1992).
  - [20] K. Miernik et al., *Nucl. Instrum. Methods Phys. Res. Sect. A* **581**, 194 (2007).
  - [21] K. Miernik et al., *Phys. Rev. Lett.* **99**, 192501 (2007).
  - [22] F. Sauli, *Nucl. Instrum. Methods A* **580**, 971 (2007).
  - [23] Ch. Ouellet and B. Singh, *Nucl. Data Sheets* **114**, 209 (2013).
  - [24] G.T. Koldste et al., *Phys. Rev. C* **87**, 055808 (2013).